Complex Formation and Redox Reactions in Copper–Pterin Cofactor Systems. Possible Relevance to Phenylalanine Hydroxylase

Yasuhiro Funahashi, Chie Kato, and Osamu Yamauchi*

Department of Chemistry, Graduate School of Science and Research Center for Materials Science, Nagoya University, Chikusa-ku, Nagoya 464-8602

(Received August 18, 1998)

With a view to understanding better the redox reactions between the metal center and the pterin cofactor in phenylalanine hydroxylase (PAH) and the effects of possible sulfur coordination to the metal center, we isolated model copper(II) complexes of 2,2′-bis(2-pyridylmethyl)amine (dpa), *S*-ethyl-*N*-(2-pyridylmethyl)aminoethanethiol (pat), and pterin-6-carboxylate (ptc), [Cu(dpa)(ptc)]·H_2O·CH_3OH (**1**), [Cu(pat)(Cl)]Cl·H_2O (**2**), and [Cu(pat)(ptc)]·$3H_2O$ (**3**), of which **1** and **3** contained ptc as a cofactor model. These binary and ternary Cu(II) complexes were studied by X-ray diffraction, spectroscopic, and electrochemical methods. Redox reactions between Cu(II) complexes ($[Cu(dpa)]^{2+}$ or **1**) and tetrahydropterins (5,6,7,8-tetrahydro-6,7-dimethylpterin ($h_4$dmp) or 5,6,7,8-tetrahydropterin-6-carboxylate ($h_4$ptc)) were also investigated by time-resolved spectroscopic methods. The molecular structures of **1**, **2**, and **3** showed that dpa and pat occupy three equatorial positions and that ptc in **1** and **3** is vertically coordinated. Complexes **2** and **3** exhibited relatively high redox potentials due to thioether sulfur coordination ($E_{1/2}$ = −0.06 and −0.18 V vs. Ag/AgCl, respectively) in contrast to $[Cu(dpa)]^{2+}$ and **1** ($E_{1/2}$ = −0.32 and −0.39 V, respectively). Coordination of $h_4$dmp and $h_4$ptc to the Cu(II) center of $[Cu(dpa)]^{2+}$ and **2** to form ternary complexes was detected by the ESR spectra with the use of the rapid mix-freeze-quenching technique; subsequent redox reactions were concluded from the absorption spectral changes.

Phenylalanine hydroxylase (PAH) is a monooxygenase, which catalyzes the conversion of L-phenylalanine to L-tyrosine by stoichiometrically using tetrahydropterin as a reducing agent and molecular oxygen as an oxygen source of hydroxylation.[1,2] PAH isolated from *Chromobacterium violaceum* (CVPAH) was found to contain 1.0 mole of type II copper per mole of enzyme.[3,4] The amino acid sequence of CVPAH is highly homologous with that of the mammalian PAHs.[5] The electron spin-echo envelope modulation studies of a wild type PAH and site-directed mutants[6] and the EXAFS study of both the oxidized and reduced forms prepared by sodium dithionite[7] suggested that two conserved histidines are bound to the Cu center in a manner similar to that of mammalian PAH.[8]

ESR studies of the CVPAH-[5-^{15}N]-6,7-dimethyl-5,6,7,8-tetrahydropterin adduct indicated that the reduced pterin cofactor directly coordinates to Cu(II) through N(5).[9] The reduction of Cu(II) center in the adduct complex was rather slow, with the first-order rate constant k_r = 0.1 min^{-1} under $h_4$dmp at saturation.[4] Tetrahydropterin and mild reducing agents such as hexacyanoferrate(II), ascorbate, and NADH were reported to be ineffective for reduction of CVPAH (strong reducing agents such as sodium dithionite and dithiothreitol (DTT) were effective for reduction of CVPAH[4]), which indicated that the type II Cu center has a rather low redox potential.[4] Preincubation of the enzyme in an assay mixture containing DTT abolished a pre-steady state lag of product accumulation, and the final velocity of catalytic turnover was remarkably faster in the presence of DTT.[4]

A previous EXAFS study indicated that dithionite reduction of CVPAH leads to a site of lower coordination number, which is most consistent with a pseudo-three-coordinate structure with two short bonds with histidine imidazoles and a long bond with the third ligand.[7] The third ligand was best fit by a sulfur or a chloride[7] according to the ESR spectral change observed upon addition of DTT to the enzyme.[4] Possible CVPAH activation processes involving sulfur coordination may require further investigation. Surprisingly, it has been shown in recent reports that DTT readily removes the copper from CVPAH and that the copper-free enzyme was fully active in catalytic turnover.[10] However, there seem to be some inconsistencies among the reports with regard to the requirement for copper, especially when the amino acid sequence and structural similarity are compared with those of mammalian PAH, which requires iron for the catalytic reaction.[1,2]

We have been studying the metal complex formation and redox reactions of metal–pterin systems as models for PAH.[11—16] We thus found the ternary and quaternary Cu(II) complex formation in solution[11,13] and determined the structures of the metal–pterin complexes including the first pterin containing ternary Cu(II) complex.[12] With a view to clarifying the Cu(II)–pterin and –tetrahydropterin binding modes and the redox reaction mechanism of the systems, as well

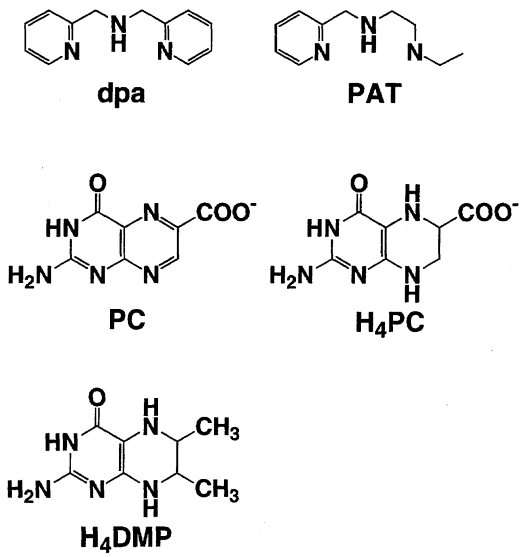

Scheme 1.

as the effect of putative sulfur coordination to the copper center, we have carried out a model study of Cu(II) complex–pterin and –tetrahydropterin systems using a tridentate N-donor ligand 2,2′-bis(2-pyridylmethyl)amine (dpa), a tridentate N,S-donor ligand *S*-ethyl-*N*-(2-pyridylmethyl)aminoethanethiol (pat), and pterin derivatives (pterin-6-carboxylate (ptc), 5,6,7,8-tetrahydropterin-6-carboxylate ($h_4$pc), and 5,6,7,8-tetrahydro-6,7-dimethylpterin ($h_4$dmp)) (Scheme 1). Three model Cu(II) complexes, [Cu(dpa)(ptc)]·H_2O·CH_3OH (**1**), [Cu(pat)(Cl)]Cl·H_2O (**2**), and [Cu(pat)(ptc)]·$3H_2O$ (**3**), have been isolated as crystals and studied by X-ray diffraction, spectroscopic, and electrochemical methods. Redox reactions between the Cu(II) complexes ($[Cu(dpa)]^{2+}$ and **2**) and tetrahydropterins have also been investigated by time-resolved spectroscopic measurements. On the basis of these results, the coordination structures, redox activities, and reaction modes of the present systems have been discussed.

Experimental

Materials. All pterin derivatives were prepared according to the literature. 5,6,7,8-Tetrahydro-6,7-dimethylpterin dihydrochloride monohydrate ($h_4$dmp·2HCl·H_2O) was prepared from 6,7-dimethylpterin (dmp) by catalytic hydrogenation with PtO_2 in 1 M HCl (M = mol dm^{-3});[17] 7,8-dihydro-6,7-dimethylpterin hydrochloride monohydrate ($h_2$dmp·HCl·H_2O) was also prepared from dmp by reduction with Zn in 0.5 M KOH;[18] ptc was prepared by oxidative cleavage of folic acid by sodium chlorate in dilute HCl;[19] 5,6,7,8-tetrahydropterin-6-carboxylic acid dihydrochloride monohydrate ($h_4$ptc·H·2HCl·H_2O) was prepared from ptc by catalytic hydrogenation with PtO_2 in CF_3COOH[20] and recrystallized from concd HCl. The purity of these pterins was checked by elemental analyses and ^{1}H NMR spectra. 2-(Ethylthio)ethylamine hydrochloride and 2,2′-bis(2-pyridylmethyl)amine (dpa) were purchased from Aldlich and TCI, respectively. $[Cu(dpa)](NO_3)_2$ was prepared by mixing equimolar amounts of $Cu(NO_3)_2$·$3H_2O$ and dpa in aqueous EtOH,[21] and the purity was checked by elemental analysis.

Preparation of *S*-ethyl-*N*-(2-pyridylmethyl)aminoethanethiol (pat): 2-(Ethylthio)ethylamine monohydrochloride (7.08 g, 50 mmol) was dissolved in 50 ml of 10 M NaOH and extracted with ether (60 ml×3). The ethereal layer was separated, dried with anhydrous sodium sulfate, and evaporated to give neutral 2-(ethylthio)ethylamine as an oil. To a solution of 2-(ethylthio)ethylamine in EtOH (100 ml) was added pyridine-2-aldehyde (5.36 g, 50 mmol). After heating the mixture at ca. 40 °C, the solvent was removed by evaporation to give a brown oil. To a solution of the oil in EtOH (100 ml) was added sodium tetrahydroborate (2.27 g, 60 mmol), and the reaction mixture was stirred overnight at room temperature. After adjusting the pH of the solution to 2 with 1 M HCl, the solvent was removed by evaporation. The brown oil obtained was dissolved in 1 M NaOH (100 ml) and extracted with ether (100 ml×3). Removal of ether by evaporation gave the crude product as an oil, which was purified by a silica gel column with ethanol as eluent. Yield 2.04 g (27%). R_f = 0.28 (on silica gel with ethanol as eluent). ^{1}H NMR ($CDCl_3$/TMS) δ = 1.25 (3H, t, J = 7.5 Hz), 2.54 (2H, q, J = 7.5 Hz), 2.73 (2H, t, J = 6.3 Hz), 2.87 (2H, t, J = 6.3 Hz), 3.94 (2H, s), 7.16 (1H, dd, J = 6.9 Hz, J' = 4.8 Hz), 7.33 (1H, d, J = 7.8 Hz), 7.65 (1H, td, J = 7.8 Hz, J' = 1.8 Hz), and 8.56 (1H, d, J = 4.8 Hz).

Preparation of Copper(II) Complexes. [Cu(dpa)(ptc)]·$3.5H_2O$ (1): A solution of ptc (0.0418 g, 2.0×10^{-4} mol) dissolved in water containing 2 equiv NaOH (0.2 M, 2 ml) was added to a stirred solution of $[Cu(dpa)](NO_3)_2$ (0.0774 g, 2.0×10^{-4} mol) in water (1 ml), when the color changed from blue to green. The green solution was kept standing for 0.5 h to give a green precipitate, which was filtered, washed with a small amount of water, and dried in vacuo. Complex **1** was obtained as a green powder. Yield 66 mg (62%). Found: C, 42.76; H, 4.02; N, 20.93%. Calcd for $C_{19}H_{23}N_8O_{6.5}Cu$: C, 42.98; H, 4.37; N, 21.10%.

[Cu(pat)(Cl)]Cl·H_2O (2): To a stirred solution of $CuCl_2$·$2H_2O$ (0.852 g, 5.0 mmol) in water (250 ml) was added a solution of pat (0.975 g, 5.0 mmol) in EtOH (250 ml), when the color of the mixture turned blue. The mixed solution was concentrated by evaporation and kept in a refrigerator overnight to give blue crystals. These were filtered, washed with a small amount of water, and dried in vacuo to give **2** as a blue powder. Yield 0.92 g (53%). Found: C, 34.88; H, 5.14; N, 8.01%. Calcd for $C_{10}H_{18}N_2OSCl_2Cu$: C, 34.44; H, 5.20; N, 8.03%.

[Cu(pat)(ptc)]·$1.5H_2O$ (3): A solution of ptc (0.23 g, 1.1 mmol) in water containing 2 equiv NaOH (0.1 M, 22 ml) was added to a stirred solution of [Cu(pat)(Cl)]Cl·H_2O (0.38 g, 1.1 mmol) in water (250 ml), when the color changed from blue to green. The solution was concentrated by evaporation and kept in a refrigerator overnight to give green crystals. These were filtered, washed with a small amount of water, and dried in vacuo to give **3** as a green powder. Yield 0.35 g (64%). Found: C, 41.87; H, 4.66; N, 19.90%. Calcd for $C_{17}H_{22}N_7O_{4.5}SCu$: C, 41.50; H, 4.51; N, 19.93%.

Spectroscopic Measurements. Electronic absorption spectra were taken on a Shimadzu UV-3101PC spectrophotometer at room temperature. X-Band ESR spectra of frozen solutions were recorded at 77 K with a JEOL RE-1X ESR spectrometer.

Electrochemical Measurements. Cyclic voltammetric measurements were carried out at room temperature under a nitrogen atmosphere by using a Hokuto Denko HB-104 function generator and an HA-104 potentio/galvanostat equipped with a Yokogawa 3086 X–Y recorder. A three-electrode system was used with a 3-mm diameter glassy carbon electrode (BAS) as the working electrode, a platinum electrode (BAS) as the counter electrode, and a Ag/AgCl electrode (BAS) as a reference electrode. The supporting electrolyte was KCl (0.1 M). The scan rate was 100 mV s^{-1} for all samples. All the potentials cited hereafter are expressed with Ag/AgCl as standard.

X-Ray Structure Determination. The single crystals of complexes **1**, **2**, and **3** suitable for X-ray analysis were obtained from methanol, aqueous EtOH, and aqueous solution as [Cu(dpa)(ptc)]·H_2O·CH_3OH (**1**), [Cu(pat)(Cl)]Cl·H_2O (**2**), and [Cu(pat)(ptc)]·$3H_2O$ (**3**), respectively. Crystal data and experimental details for these complexes are summarized in Table 1. Diffraction data were collected with a Rigaku AFC-5R four-circle automated diffractometer at 295 K. The reflection intensities were monitored by three standard reflections for every 150 measurements. Such monitoring indicated that the decays of intensities for these crystals were not significant. Reflection data were corrected for Lorentz and polarization effects. Absorption corrections were empirically applied in all the crystals. Independent reflections with $|F_o| \geq 3\sigma(|F_o|)$ were used for the structure determinations. The calculations were performed on an SGI IRIS Indigo 4D/RPC computer by using the program system teXsan.[22] The structures were solved by the direct method and refined anisotropically for non-hydrogen atoms by the full-matrix least-squares method, while most hydrogen atoms were located at their standard geometries by calculation and some were fixed at observed peak positions by difference Fourier synthesis. All refinements were continued until each shift/error in the final cycle attained a minimum value (0.04, 0.01, and 0.48 for **1**, **2**, and **3**). Atomic scattering factors and anomalous dispersion terms were taken from the literature.[23] The final R and R_w values were 0.055 and 0.055 for **1**, 0.023 and 0.035 for **2**, and 0.050 and 0.059 for **3**, respectively. The weighting scheme $w = 1/\sigma^2(F_o)$ was employed for the three crystals. The final difference Fourier maps did not show any significant peaks except the ghost peaks close to metal atoms. The selected bond lengths and angles for the three complexes are listed in Table 2. Tables of the final parameters for all non-hydrogen atoms and positions of hydrogen atoms, bond lengths and angles, torsion angles, and observed and calculated structure factor amplitudes are deposited as Document No.72006 at the Office of the Editor of Bull. Chem. Soc. Jpn.

Table 2. Selected Bond Distances (Å) and Angles (°) for [Cu(dpa)(ptc)]·H_2O·CH_3OH (**1**), [Cu(pat)(Cl)]Cl·H_2O (**2**), and [Cu(pat)(ptc)]·$3H_2O$ (**3**)

Complex	1	2	3
Cu–O(4)	2.459(7)	—	2.499(8)
Cu–N(5)	2.009(8)	—	1.977(9)
Cu–O(61)	2.347(7)	—	2.356(8)
Cu–N(1*)	1.989(8)	2.027(2)	2.04(1)
Cu–N(2*)	2.008(8)	2.001(3)	1.978(10)
Cu–N(3*)	2.025(8)		
Cu–S(1*)	—	2.3691(8)	2.405(5)
Cu–Cl(1)	—	2.251(1)	—
Cu–Cl(2)	—	2.659(1)	—
N(3)–C(4)	1.33(1)	—	1.36(1)
C(4)–O(4)	1.26(1)	—	1.24(1)
O(4)–Cu–N(5)	74.3(3)	—	73.9(3)
N(5)–Cu–O(61)	73.6(3)	—	75.7(3)
N(1*)–Cu–S(1*)	—	161.95(9)	166.2(3)
N(5)–Cu–N(2*)	168.0(4)	—	178.0(5)
Cl(1)–Cu–N(2*)	—	170.08(8)	—

ESR Rapid Mix-Freeze-Quenching Technique and Stopped Flow-Rapid Mixing-Rapid Scanning Technique. Each sample solution was made by mixing a Cu(II) complex and a tetra-

Table 1. Crystallographic Data for [Cu(dpa)(ptc)]·H_2O·CH_3OH (**1**), [Cu(pat)(Cl)]Cl·H_2O (**2**), and [Cu(pat)(ptc)]·$3H_2O$ (**3**)

	1	2	3
Formula	$CuC_{20}H_{22}N_8O_5$	$CuC_{10}H_{18}N_2OSCl_2$	$CuC_{17}H_{25}N_7O_6S$
Formula weight	517.99	348.78	519.03
Color	Green	Blue	Green
Crystal size /mm	0.10 ×0.05 × 0.03	0.45 × 0.15 × 0.10	0.13 × 0.10 × 0.03
Crystal system	Triclinic	Monoclinic	Monoclinic
Space group	$P\bar{1}$	$P2_1/n$	$C2/c$
a/Å	10.629(2)	10.006(4)	17.651(3)
b/Å	11.660(2)	10.694(8)	14.163(3)
c/Å	10.403(2)	13.549(4)	18.912(6)
α/deg.	110.46(1)	—	—
β/deg.	111.64(2)	100.38(3)	106.27(2)
γ/deg.	75.79(2)	—	—
V/Å^3	1112.7	1426.1	4538
Z	2	4	8
D_c/g cm^{-3}	1.546	1.624	1.519
Radiation	Cu $K\alpha$ (1.54178 Å)	Cu $K\alpha$ (1.54178 Å)	Cu $K\alpha$ (1.54178 Å)
μ/cm^{-1}	18.32	68.65	26.48
F(000)/e	534.0	716.0	2152.0
Scan method	ω–2θ	ω–2θ	ω–2θ
$2\theta_{max}$/deg.	120.1	120.2	120.2
Scan speed/deg.min^{-1}	4.0	16.0	4.0
Scan range/deg.	1.57+0.30 tan θ	1.84+0.30 tan θ	1.37+0.30 tan θ
No. reflections obsd.	2908	1979	3058
No. reflections used	1406	1499	1130
R[a)]	0.055	0.023	0.050
R_w[a)]	0.055	0.035	0.059

a) $R = \sum||F_o| - |F_c||/\sum|F_o|$; $R_w = [\sum w(|F_o| - |F_c|)2/\sum w|F_o|^2]^{1/2}$; $w = 1/\sigma^2(F_o)$.

hydropterin in 50 mM Hepes buffer solution containing 1 M acetonitrile[24,25] at pH 7 (ionic strength I = 0.1 M) (Hepes = 2-(4-(2-hydroxyethyl)-1-piperazinyl)ethanesulfonic acid). The pH and I were adjusted by NaOH and NaCl. The concentrations of the Cu(II) complex and tetrahydropterin were 1 mM. The ESR spectra of the reaction intermediates were measured by a rapid mix-freeze-quenching technique originally described by Bray.[26] One brief modification in freezing sample solutions was introduced to this procedure. The mist of the mixed solution was sprayed under an anaerobic condition on the inner surface of a copper cylinder, which had been previously cooled by liq. N_2. The Cu(II) concentration was determined by double integration of spectra[27] by using **2** as a standard. Electronic absorption spectral changes with time were measured at 25 °C by a Unisoku stopped flow-rapid mixing-rapid scanning system equipped with D_2 and W lamps.

High-Performance Liquid Chromatography (HPLC). A Shimadzu LC-10A high-performance liquid chromatograph, a Shimadzu SPD-M10AV photodiode array UV-vis spectrophotometer equipped with D_2 and W lamps, and a quartz flow cell (1 mmϕ × 10 mm) were used. A Shiseido Capcel pack C18 UG 120A reverse-phase column having octadecyl groups on the fixed phase (5 mm, 4.6 mmϕ × 250 mm) was employed for separation and identification of the reaction products, which were eluted at 1.0 ml min^{-1} with 90 w/w% EDTA·2Na (5 mM)–10 w/w% acetonitrile.

Results and Discussion

Molecular Structures of [Cu(dpa)(ptc)]·H_2O·CH_3OH (1), [Cu(pat)(Cl)]Cl·H_2O (2), and [Cu(pat)(ptc)]·$3H_2O$ (3). The molecular structure of **1**, also showing the atomic numbering scheme, is given in Fig. 1, which shows that the Cu(II) ion has an axially distorted octahedral geometry due to the Jahn–Teller effect. In this structure, ptc is vertically bound to the Cu(II) ion in the same manner as in [Cu(bpy)(ptc)(H_2O)] (bpy = 2,2′-bipyridine).[12] The two pyridine nitrogen and secondary amine nitrogen atoms of dpa, and the N(5) atom of ptc occupy the four equatorial positions with the two oxygen atoms of ptc occupying the axial positions (Cu–N(1*) = 1.989(8), Cu–N(2*) = 2.008(8), Cu–N(3*) = 2.025(8), Cu–O(4) = 2.459(7), Cu–N(5) = 2.009(8), Cu–O(61) = 2.347(7) Å). The molecular structure of **2** is shown in Fig. 2, with the atomic numbering scheme. The Cu(II) ion has a five-coordinate square-pyramidal geometry, where the three donor atoms of pat, a pyridine nitrogen, a secondary amine nitrogen, and a thioether sulfur, and one chloride ion are equatorially bound with typical bond lengths (Cu–N(1*) = 2.027(2), Cu–N(2*) = 2.001(3), Cu–S(1) = 2.3691(8), and Cu–Cl(1) = 2.251(1) Å). The Cu–S(1) bond length is somewhat shorter for copper–thioether bonds (2.347—2.470 Å).[28] The axially coordinated chloride ion is located at a long distance from Cu(II) (Cu–Cl(2) = 2.659(1) Å). The molecular structure of **3** (Fig. 3) shows that the Cu(II) ion is in an axially distorted octahedral geometry, and the ptc molecule is vertically coordinated to Cu(II) as in **1** by replacing the two chloride ions of **2** (Cu–N(1*) = 2.04(1), Cu–N(2*) = 1.978(10), Cu–S(1) = 2.405(5), Cu–O(4) = 2.499(8), Cu–N(5) = 1.977(9), and Cu–O(61) = 2.356(8) Å).

The axial bonds, Cu–O(4) and Cu–O(61) in **1** and **3**, are elongated, as found in [Cu(bpy)(ptc)(H_2O)].[12] The observed Cu–O(4) bonds (2.459(7), 2.499(8), and 2.499(3) Å for **1**, **3**, and [Cu(bpy)(ptc)(H_2O)],[12] respectively) are longer than the bond for horizontally coordinated pterinate

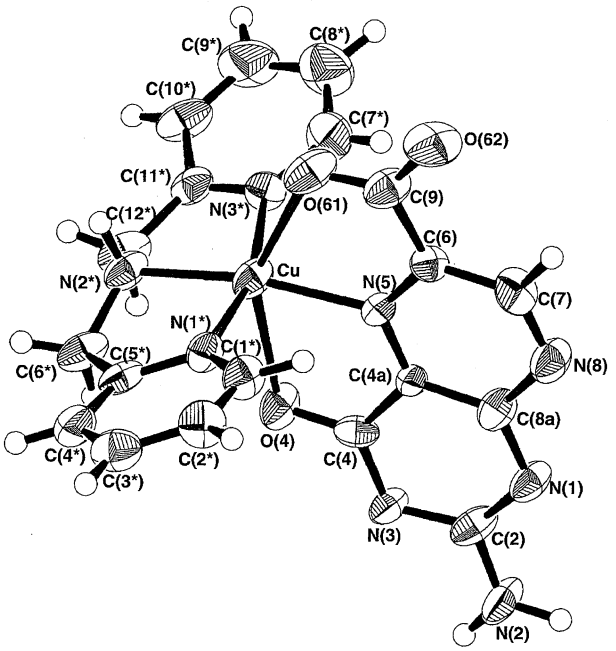

Fig. 1. Molecular structure of [Cu(dpa)(ptc)]·H_2O·CH_3OH (**1**) showing the atomic numbering scheme. Thermal ellipsoids are drawn at the 50% probability level.

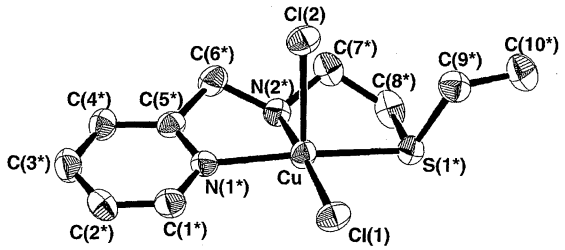

Fig. 2. Molecular structure of [Cu(pat)(Cl)]Cl·H_2O (**2**) showing the atomic numbering scheme. Thermal ellipsoids are drawn at the 50% probability level.

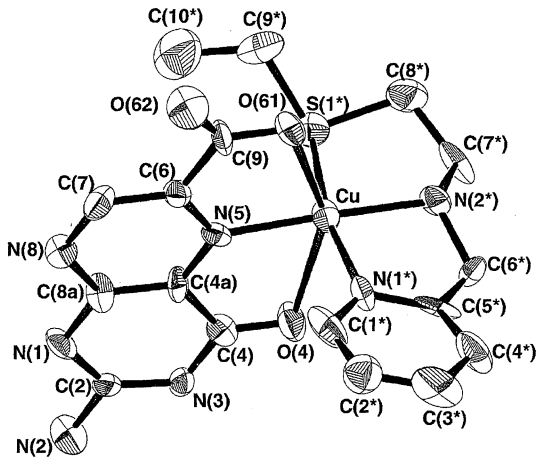

Fig. 3. Molecular structure of [Cu(pat)(ptc)]·$3H_2O$ (**3**) showing the atomic numbering scheme. Thermal ellipsoids are drawn at the 50% probability level.

(1.969(5) Å for $[Cu(ndmp)_2(MeOH)_2]$ (ndmp = 2-(dimethylamino)-4(3*H*)-pteridinone)[16]). This order is correlated with the order of the C(4)–O(4) bond length (neutral pterin (1.221(8) Å for euglenapterin[29]) < vertically coordinated ptc (1.26(1), 1.24(1), and 1.238(5) Å for **1**, **3**, and $[Cu(bpy)(ptc)(H_2O)]$,[12] respectively) < horizontally coordinated pterinate (1.278(8) Å for $[Cu(ndmp)_2(MeOH)_2]$[16]). Simultaneously, the N(3)–C(4) bond length decreases in the order, neutral pterin (1.394(9) Å for euglenapterin[29]) > vertically coordinated ptc (1.33(1), 1.36(1), and 1.339(5) Å for **1**, **3**, and $[Cu(bpy)(ptc)(H_2O)]$,[12] respectively) > horizontally coordinated pterinate (1.322(8) Å for $[Cu(ndmp)_2(MeOH)_2]$[16]). The N(3)–C(4) and C(4)–O(4) bond lengths change with the deprotonation and coordination of the N(3)–C(4)–O(4) moiety.[16] These data indicate that ptc is deprotonated at the N(3) position and that the axial Cu–O(4) bond is somewhat weaker than the equatorial one of horizontally coordinated pterinate in $[Cu(ndmp)_2(MeOH)_2]$.[16]

Although the crystal structures of **1** and **3** show that $[Cu(dpa)]^{2+}$ and **2** structurally allow ptc to coordinate to the Cu(II) center, the binding site for the ptc ring is narrow and crowded due to the coordination of the first ligand. The two pyridine rings of dpa in **1** are situated near the N(5)–C(6)–C(9) moiety of ptc, the shortest distance being N(5)–H(C(1*)) = 2.84 Å. In the structure of **3**, the pyridine ring and the ethyl group of the terminal ethylthio group approach the N(5)–C(6)–C(9) moiety with the shortest distances N(5)–H(C(1*)) = 2.87 and N(5)–H(C(10*)) = 3.01 Å. These nonbonding distances are slightly longer than the corresponding sums of the van der Waals radii. Because of the strain due to the steric hindrance, the coordination bond lengths of the Cu-pat moiety in **3**, the Cu–N(1*) and Cu–S(1*) bonds, are significantly increased from 2.027(2) and 2.3691(8) Å in **2** to 2.04(1) and 2.405(5) Å in **3**, respectively (Table 2).

Electronic Absorption and ESR Spectra of 1, 2, and 3. The electronic absorption and ESR spectral data for $[Cu(dpa)](NO_3)_2$, **1**, **2**, and **3** are given in Table 3. Complex **2** exhibited three distinct absorption peaks, of which the most intense one at 328 nm is assigned to the σ(S)→d(Cu) charge transfer,[30,31] and the bands at 653 and 255 nm are assigned to the d–d transition and π–π* transition of the pyridine ring, respectively. The latter was also exhibited in the $[Cu(dpa)]^{2+}$ spectrum at 252 nm. The intense σ(S)→d(Cu) CT band indicates that **2** in solution has the thioether sulfur atom in an equatorial position of the square planar geometry.[31] Complex **3** exhibited four distinct absorption peaks and one broad band centered at ca. 340 nm, which is assigned to the σ(S)→d(Cu) CT shifted to the lower energy region due to ptc coordination. The σ(S)→d(Cu) CT band and the π–π* transition band of pyridine were obscured by the strong π–π* transition bands of ptc. The bands of deprotonated ptc at 263 and 363 nm were bathochromically shifted to 278 and 380 nm for **1**, and 279 and 377 nm for **3**, respectively, due to its coordination.[16] The d–d peaks for $[Cu(dpa)]^{2+}$ and **2** at 653 nm were shifted to 612 nm, and the shoulder peak characteristic of a five-coordinate geometry appeared at a longer wavelength (ca. 850 and 841 nm for **1** and **3**, respectively) due to axial coordination by ptc. The intense absorptivities of the d–d bands for **2** and **3** may be attributed to contribution of the π(S)→d(Cu) CT components in the visible region.[31,32]

These absorption spectral data support the conclusion that **1**, **2**, and **3** in solution maintain the same coordination geometries as those revealed in the solid state, where the sulfur atom remains coordinated in the equatorial position and ptc is vertically coordinated (Figs. 1, 2, and 3).

The ESR spectra of $[Cu(dpa)]^{2+}$, **1**, **2**, and **3** measured in solution at 77 K gave signals of axial symmetry in a $d_{x^2-y^2}$ ground state ($g_{\parallel} > g_{\perp}$) (Table 3). The $g_{\parallel}$ values of **1** and **3** were smaller and the $|A_{\parallel}|$ values were larger than the corresponding values of $[Cu(dpa)]^{2+}$ and **2**, due to the equatorial coordination of N(5) of ptc. These changes are consistent with the tendency that an additional nitrogen atom in the equatorial positions will cause the $g_{\parallel}$ value to decrease and the $|A_{\parallel}|$ value to increase.[33–36] The difference

Table 3. Electronic and ESR Spectral Data for $[Cu(dpa)](NO_3)_2$, $[Cu(dpa)(ptc)]\cdot H_2O\cdot CH_3OH$ (**1**), $[Cu(pat)(Cl)]Cl\cdot H_2O$ (**2**), and $[Cu(pat)(ptc)]\cdot 3H_2O$ (**3**)

	ESR(77K)			Absorption						
Complex	$g_{\perp}$	$g_{\parallel}$	$\|A_{\parallel}\|$/mT	$\lambda_{max}(\varepsilon)$/nm $M^{-1}cm^{-1}$						pH
[Cu(dpa)]	2.06	2.26	17.5	252 (9480)				653 (93)		6.3
1	2.05	2.23	18.7		278 (25400)		380 (7980)	612 (92)	ca. 850 (21)	6.9
2	2.05	2.24	17.5	255 (5900)		328 (4000)		653 (180)		5.7
3	2.05	2.20	17.7		279 (27000)	ca. 340 (ca. 8000)	377 (8600)	612 (180)	841 (43)	7.1
ptc^{2-}	—	—	—		263 (21600)		363 (9380)			9.4
h_4ptc	—	—	—			304 (7570)[a]				7.0[a]

a) Measured by the rapid-scanning system in the range 275—475 nm. Prepared in 50 mM Hepes buffer solution containing 1 M acetonitrile (pH 7.0, I = 0.1).

of the $|A_{\parallel}|$ values between **2** and **3** appeared to be negligible, because axial coordination decreases the unpaired electron density in the Cu(II) plane to give a small $|A_{\parallel}|$ value.[36—39] Replacement of hard donor atoms with soft donor atoms in planar Cu(II) complexes has been reported to decrease both $g_{\parallel}$ and $|A_{\parallel}|$ values by delocalization of the unpaired electron density away from the Cu nucleus, due to increased covalency of the metal–ligand bond.[35,36,39] The $g_{\parallel}$ and $|A_{\parallel}|$ values for **2** and **3** are different from those for $[Cu(dpa)]^{2+}$ and **1** mostly according to this tendency, supporting the equatorial coordination of a sulfur atom in place of a pyridine nitrogen atom.

These ESR spectral features are also consistent with the geometries found in the crystal structures (Figs. 1, 2, and 3).

Electrochemical Properties. Cyclic voltammetric data of $[Cu(dpa)](NO_3)_2$, **1**, **2**, and **3** are listed in Table 4. These complexes exhibited reversible or quasi-reversible cyclic voltammograms[40] with a pair of cathodic and anodic waves of Cu(II)/Cu(I). Coordination of ptc to the copper center of $[Cu(dpa)]^{2+}$ ($E_{1/2} = -0.32$ V) and **2** (−0.06 V) caused a negative shift of the redox potentials for Cu(II)/Cu(I) ($E_{1/2} = -0.39$ and −0.18 V for **1** and **3**, respectively). The ternary complex rather than the binary complex stabilizes Cu(II) state. The remarkable differences in the $E_{1/2}$ values detected between $[Cu(dpa)]^{2+}$ (−0.32 V) and **2** (−0.06 V) and between **1** (−0.39 V) and **3** (−0.18 V) are ascribed to the replacement of a pyridine ring of dpa with a thioether sulfur with a greater π-acceptor character,[39] which stabilizes the Cu(I) state.

Time Course of Absorption Spectral Changes for Cu(II) Complex–Tetrahydropterin Systems. The reactions in the Cu(II) complex–tetrahydropterin systems in 50 mM Hepes buffer solution containing 1 M acetonitrile (pH 7.0, $I = 0.1$) were monitored by the stopped flow-rapid mixing-rapid scanning technique in the visible and UV regions.

(a) $[Cu(dpa)]^{2+}$–Tetrahydropterin Systems. In both the $[Cu(dpa)]^{2+}$–$h_4$ptc and –$h_4$dmp systems, no absorption spectral changes were observed in 0.5 s, and the tetrahydropterins were ineffective reducing agents for $[Cu(dpa)]^{2+}$. The $[Cu(dpa)]^{2+}$–$h_4$ptc system exhibited the d–d band at 659 nm with a broad band at a longer wavelength (ca. 880 nm). The 659 nm band was slightly shifted from 654 nm observed for $[Cu(dpa)]^{2+}$ in the same medium. It is known on the basis of the solution equilibrium studies of the Cu(II)–X–ptc systems[13] that more than 70% of Cu(II) present in solution forms a ternary complex [Cu(X)(ptc)] (X = ethylenediamine, bpy, 1,10-phenanthroline, 2,2′ : 6′,2″-terpyridine, and diethylenetriamine) at pH 7 under the condition of [Cu(II)] = [X] = [ptc] = 1 mM. Since the coordinating atoms of $h_4$ptc are similar to those of ptc, $h_4$ptc should be as effective a ligand as ptc, but probably because of only one equatorial position available in $[Cu(dpa)]^{2+}$ and the tetrahedral structure around N(5) in $h_4$ptc, it may be weakly coordinated to Cu(II) owing to steric hindrance. In the $[Cu(dpa)]^{2+}$–$h_4$dmp system, the 654 nm band of $[Cu(dpa)]^{2+}$ was shifted to a higher energy level (651 nm), which may be simply ascribed to N(5) atom coordination.

(b) $[Cu(pat)]^{2+}$–Tetrahydropterin Systems. The spectral changes for the **2**–$h_4$ptc and –$h_4$dmp systems are shown in Figs. 4 and 5, respectively. The intensity of the absorption band in the visible region for the **2**–$h_4$ptc system diminished immediately after mixing, as shown in Fig. 4a. In the UV region, the peak of $h_4$ptc at 304 nm initially diminished in ca. 0.5 s, and then the absorbance at 300—400 nm increased (Fig. 4b). This is probably due to formation of oxidized pterins such as 7,8-dihydropterin (Scheme 2). Although an isosbestic point was observed at 438 nm during the slow reaction step, initial changes were too fast to follow. For the **2**–$h_4$dmp system, two sequential changes were observed in the visible region. First, a blue shift of the 650 nm peak to 585 nm with concomitant intensity increase was observed for ca. 10 s, and then the whole band in the visible region slowly decreased (Fig. 5a). Upon addition of $h_4$dmp to **2**, the solution turned dark blue due to intense absorption in the visible region, whereas the Cu(I)–pat complex prepared by electrochemical reduction of **2** showed no such band in the visible region (data not shown). In this connection, a similar strong band has been reported previously for Cu(II) complex–tetrahydropterin systems, but the relevant species have not been well characterized.[41] In the UV region, the increase and subsequent decrease in absorbance at 340—450 nm were observed due to oxidation of $h_4$dmp (Fig. 5b), whose reaction mixture was found by HPLC to contain $h_4$dmp and 7,8-dihydro-6,7-dimethylpterin ($h_2$dmp) in approximately equal amounts (39.5 and 36.3% yields, respectively, based on $h_4$dmp initially used). The difference spectrum measured in the subsequent step exhibited a peak centered at 333 nm, which is characteristic of formation of $h_2$dmp.[42] The initial increase until ca. 10 s after mixing and subsequent decrease of the absorbance at 340—450 nm may be attributed to formation and isomerization of the quinonoid dihydropterin (Scheme 2).[42,43] The redox reaction in the **2**–$h_4$dmp system was remarkably fast, as described below, and Cu(II) must be mostly reduced within ca. 10 s (the final concentration of

Table 4. Electrochemical Parameters for $[Cu(dpa)](NO_3)_2$, $[Cu(dpa)(ptc)]\cdot H_2O\cdot CH_3OH$ (**1**), $[Cu(pat)(Cl)]Cl\cdot H_2O$ (**2**), and $[Cu(pat)(ptc)]\cdot 3H_2O$ (**3**) (V vs. Ag/AgCl)[a]

Complex	E_{pc}/V	E_{pa}/V	$E_{1/2}$/V	ΔE_p/V	pH
$[Cu(dpa)](NO_3)_2$	−0.36	−0.28	−0.32	0.079	5.4
1	−0.45	−0.33	−0.39	0.121	7.3
2	−0.09	−0.03	−0.06	0.058	5.7
3	−0.24	−0.11	−0.18	0.132	7.1

a) The supporting electrolyte was KCl (0.1 M). Scan rate; 100 mV s^{-1}.

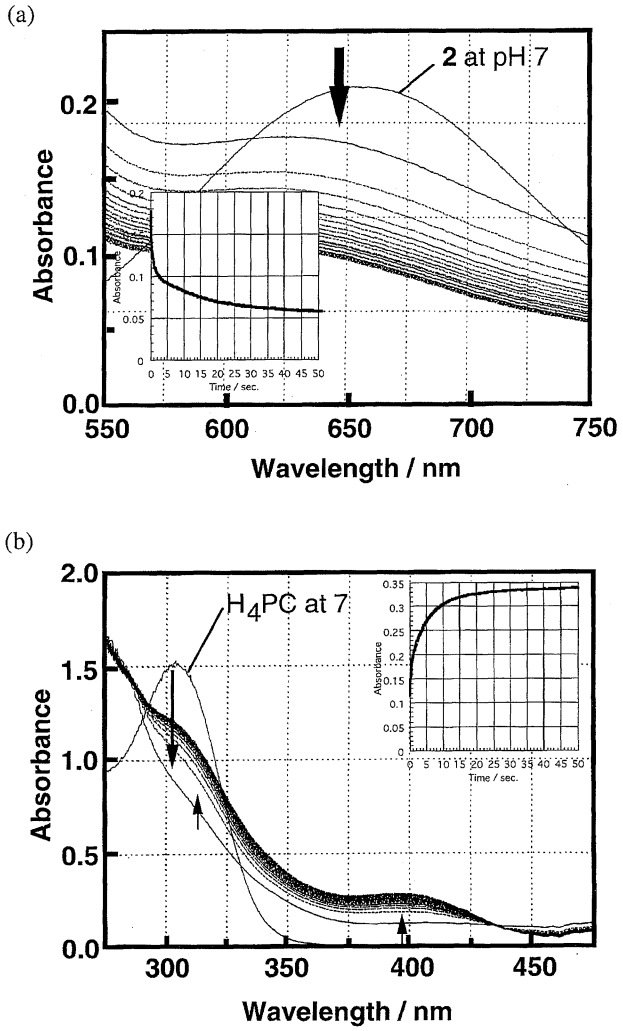

Fig. 4. Time course of the electronic absorption spectral changes for 1 : 1 **2**–$h_4$ptc (a) in the visible region and (b) in the UV region. The insets show the changes of absorbances (a) at 624 nm and (b) at 391 nm.

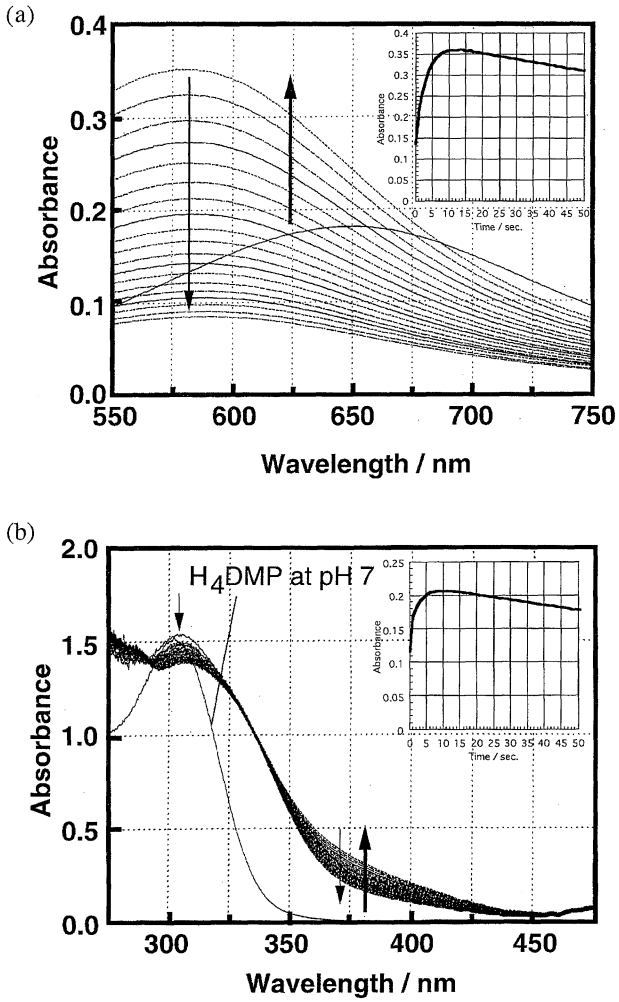

Fig. 5. Time course of the electronic absorption spectral changes for 1 : 1 **2**–$h_4$dmp system (a) in the visible region and (b) in the UV region. The insets show the changes of absorbances (a) at 585 nm and (b) at 400 nm.

Cu(II) state was estimated by ESR spectral intensity to be 29 and 6% for $h_4$ptc and $h_4$dmp, respectively). Therefore, the strong band in the visible region may be due to the CT arising from Cu(I)–quinonoid dihydropterin bonding. In the $[Cu(dpa)]^{2+}$–tetrahydropterin systems, no absorption spectral changes were observed due to stabilization of the Cu(II) state, but, in **2**–tetrahydropterin systems, drastic absorption spectral changes were observed owing to the redox reactions.

Formation of Ternary Complexes with Tetrahydropterins. Adduct formation in the Cu(II) complex–tetrahydropterin systems in 50 mM Hepes buffer solution containing 1 M acetonitrile (pH 7) has been studied by the ESR measurements using the rapid mix-freeze-quenching technique. The systems in this medium exhibited somewhat different ESR spectra from those in H_2O (pH ca. 6) due to coordination of acetonitrile.[24,25] Addition of tetrahydropterins to these systems gave rise to further ESR spectral changes, which resulted from the geometrical changes accompanying formation of the ternary complexes. The Cu(II) concentrations of these ternary complexes were estimated by ESR signal integration to be ca. 90% for **2**–$h_4$ptc and ca. 35% for **2**–$h_4$dmp on the basis of the total copper used. Table 5 shows that the observed ESR spectral features in $[Cu(dpa)]^{2+}$–$h_4$ptc, **2**–$h_4$ptc, and **2**–$h_4$dmp were of axial symmetry in a $d_{x^2-y^2}$

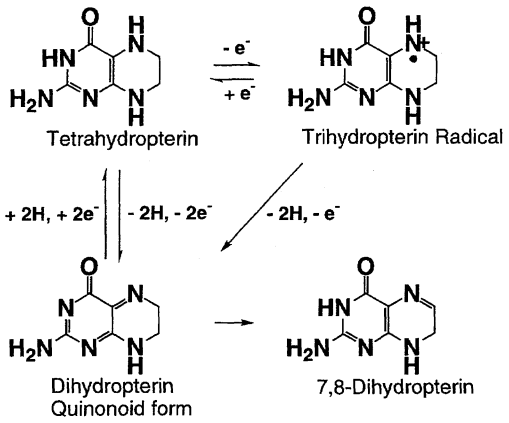

Scheme 2.

Table 5. ESR Spectral Parameters for Cu(II) Complex–Tetrahydropterin Systems at 77 K by Rapid Mix-Freeze-Quenching Technique

Complex	$g_\perp$	$g_\parallel$	$\lvert A_\parallel \rvert$/mT	pH[a]
$[Cu(dpa)]^{2+}$ + $h_4$ptc	2.06	2.24	17.7	7.0
2 + $h_4$ptc	2.06	2.24	18.0	7.0
2 + $h_4$dmp	2.06	2.22	17.8	7.0
CVPAH[b]	2.06	2.32	14.5	6.5
CVPAH-$h_4$dmp adduct[b]	2.06	2.27	15.7	6.5

a) Measured in 1 M acetonitrile and 50 mM Hepes buffer solution (pH 7.0). b) Refs. 4 and 9.

ground state ($g_\parallel > g_\perp$) at 77 K. The $[Cu(dpa)]^{2+}$–$h_4$dmp system exhibited a broad signal at g = ca. 2, which may be explained by the presence of a monomer–dimer equilibrium in the frozen solution[44] (data not shown).

The $[Cu(dpa)]^{2+}$–$h_4$ptc and **2**–$h_4$ptc systems showed analogous ESR signals with $g_\parallel$ = 2.24 and $|A_\parallel|$ = 17.7 mT and $g_\parallel$ = 2.24 and $|A_\parallel|$ = 18.0 mT, respectively. In the ternary complexes formed, Cu(X)($h_4$ptc) (X = dpa and pat), almost no differences are found in these parameters, implying that Cu(II) ions in these complexes have nearly the same coordination geometries. Considering that **3** exhibited different parameters from those of **1** due to the sulfur coordination, the donor groups in the Cu(II) plane might have been changed to accommodate $h_4$ptc, that is, the thioether sulfur of pat and one pyridine of dpa might no longer be equatorially coordinated due to steric hindrance between $h_4$ptc and X. Indeed, the $g_\parallel$ value of the ternary complexes increased in the order: **3** (2.20) < **1**(2.23) < Cu(X)($h_4$ptc) (X = dpa and pat) (2.24). The $g_\parallel$ value for **2**–$h_4$dmp ($g_\perp$ = 2.05, $g_\parallel$ = 2.22, $|A_\parallel|$ = 18.3 mT) was larger than that of **3**, suggesting that the thioether sulfur of pat in Cu(pat)($h_4$dmp) also lies apart from the equatorial position due to coordination of $h_4$dmp. When two coordination sites are available, $h_4$dmp may coordinate horizontally to the Cu(II) plane as in $[Cu(ndmp)_2(MeOH)_2]$.[16]

The ESR spectral changes due to addition of tetrahydropterins to $[Cu(dpa)]^{2+}$ and **2** indicate that tetrahydropterins coordinate to the Cu(II) center to form the corresponding ternary complexes, Cu(X)(tetrahydropterin), with possible changes in the equatorial coordination of the tridentate ligands due to accommodation of tetrahydropterin. From the absorption spectral observations as described in the preceding section and the previous observations,[15,45] we propose the reaction pathways for the Cu^{II}(X)–tetrahydropterin systems which are shown in Scheme 3, where a ternary complex is rapidly formed and a one-electron redox reaction initially takes place, generating Cu^{I}(X) and a trihydropterin radical; the radical should then readily disproportionate to the corresponding tetrahydro- and dihydropterins, the latter of which reacts with Cu^{I}(X) to form Cu^{I}(X)(dihydropterin) in the quinonoid form (blue) and then in the 7,8-dihydro form. The fact that a considerable amount (39.5%) of tetrahydropterin was present after the reaction further supports the proposed mechanism. Formation of the ternary complex Cu^{II}(X)(tetrahydropterin) may stabilize the Cu(II) state and thus hinder the redox reaction.

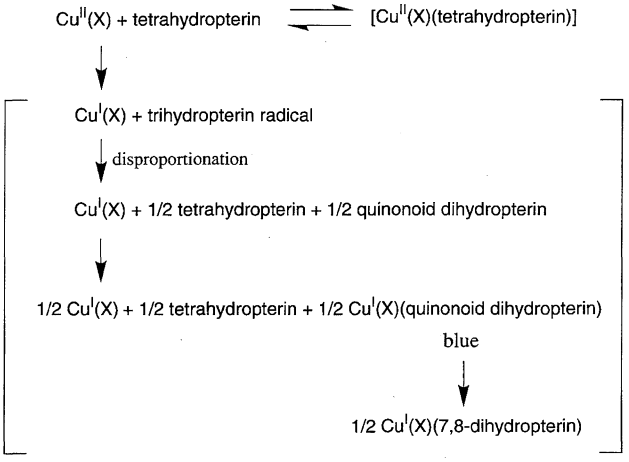

Scheme 3. Proposed reaction pathways.

Biological Implication. The present spectroscopic studies have revealed that the ternary complexes with tetrahydropterins were formed in the Cu(II) complex–tetrahydropterin systems. The ternary complexes exhibited ESR signals of axial symmetry in the $d_{x^2-y^2}$ ground state ($g_\parallel > g_\perp$), where the electron spin is localized in the Cu(II) plane. The CVPAH–$h_4$dmp adduct has also been reported to exhibit a signal of axial symmetry in a $d_{x^2-y^2}$ ground state,[9] where the $g_\parallel$ value (2.27) is larger and the $|A_\parallel|$ value (15.8 mT) is smaller than the corresponding values for Cu(dpa)($h_4$ptc), Cu(pat)-($h_4$ptc), and Cu(pat)($h_4$dmp). This may indicate a less electron-donating equatorial coordination and/or a further axial coordination to the Cu(II) center of CVPAH. It is known that the two-electron redox potential of $h_4$dmp is ca. −0.05 V at pH 7,[43,46] and that the Cu(II) center of the CVPAH–$h_4$dmp adduct was not reduced very much.[4] Therefore, the redox potential is negatively shifted in the order: **2** ($E_{1/2}$ = −0.06 V) > CVPAH > $[Cu(dpa)]^{2+}$ ($E_{1/2}$ = −0.32 V).

On the basis of the Cu(II) state in the **2**–tetrahydropterin system estimated from the rapid mix-freeze-quenching experiment, $h_4$dmp is concluded to be a more efficient reducing agent than $h_4$ptc, whose ligating carboxylate group at the 6-position would stabilize the corresponding ternary complex. When the dead time of the rapid mix–freeze–quenching technique is assumed to be 50 —100 ms, the second order rate constant is estimated to be 1.9—3.7×10^4 M^{-1} s^{-1} for **2**–$h_4$dmp. This reduction rate is comparable with that for mammalian PAH by 5,6,7,8-tetrahydro-6-methylpterin (the second-order rate constant k_r = 2×10^4 M^{-1} s^{-1}).[47]

Conclusion

In order to understand the metal–pterin cofactor interactions, we synthesized and characterized model copper(II) complexes, [Cu(dpa)(ptc)]·H_2O·CH_3OH (**1**), [Cu(pat)(Cl)]-Cl·H_2O (**2**), and [Cu(pat)(ptc)]·$3H_2O$ (**3**) and investigated the mechanisms of redox reactions in the $[Cu(X)]^{2+}$ (X = dpa and pat)–tetrahydropterin ($h_4$pc and $h_4$dmp) systems. The molecular structures of **1**, **2**, and **3** showed that the tridentate ligands, dpa and pat, occupied three equatorial positions with ptc vertically coordinated in **1** and **3**. The redox potentials for complexes **2** and **3** ($E_{1/2}$ = −0.06 and −0.18 V, respectively) were more positive than those for $[Cu(dpa)]^{2+}$ and complex **1** ($E_{1/2}$ = −0.32 and −0.39 V, respectively), reflecting the effect of sulfur coordination. $h_4$ptc and $h_4$dmp coordinated to the Cu(II) center of $[Cu(dpa)]^{2+}$ and **2** to form the corresponding ternary complexes, and the ternary complexes of **2** with tetrahydropterins were redox active, while those of $[Cu(dpa)]^{2+}$ were poorly reactive.

The present studies have shown the Cu(II) binding modes of oxidized and reduced pterins and redox activities of $Cu^{II}(X)$–tetrahydropterin systems, which are dependent on the $Cu^{II}(X)$ complex structure. These findings may provide information on the reactions of aromatic amino acid hydroxylases.

We are grateful to Professor Emeritus Sadao Matsuura, Nagoya University, for the synthesis of pterin derivatives. We also thank Professor Shigenobu Funahashi,Nagoya University, for the use of the rapid-mixing and rapid-scanning systems. This work was supported by a Grant-in-Aid for Scientific Research (No. 09304062) and that on Priority Areas (Metal-assembled Complexes, No. 10149219) from the Ministry of Education, Science, Sports and Culture, for which we express our thanks. A predoctoral fellowship to Y. F. from the Japan Society for the Promotion of Science is gratefully acknowledged.

References

1) a) S. Kaufman and D. B. Fisher, in "Molecular Mechanisms of Oxygen Activation," ed by O. Hayaishi, Academic Press, New York (1974), p. 285; b) S. Kaufman, *Adv. Enzymol. Relat. Areas Mol. Biol.*, **67**, 77 (1993).

2) R. Shiman, in "Folates and Pterins: Chemistry and Biochemistry of Pterins,"ed by R. L. Blakley and S. J. Benkovic, John Wiley & Sons, New York (1985), Vol. 2, p. 179.

3) H. Nakata, T. Yamauchi, and H. Fujisawa, *J. Biol. Chem.*, **254**, 1829 (1979).

4) S. O. Pember, J. J. Villlafranca, and S. J. Benkovic, *Biochemistry*, **25**, 6611 (1986).

5) A. Onishi, L. J. Liotta, and S. J. Benkovic, *J. Biol. Chem.*, **266**, 18454 (1991).

6) a) J. McCracken, S. O. Pember, S. J. Benkovic, J. J. Villafranca, R. J. Miller, and J. Peisach, *J. Am. Chem. Soc.*, **110**, 1069 (1988); b) S. Balasubramanian, R. T. Carr, C. J. Bender, J. Peisach, and S. J. Benkovic, *Biochemistry*, **33**, 8532 (1994).

7) N. J. Blackburn, R. W. Strange, R. T. Carr, and S. J. Benkovic, *Biochemistry*, **31**, 5298 (1992).

8) a) K. E. Goodwill, C. Sabatier, C. Marks, R. Raag, P. F. Fitzpatrick, and R. C. Stevens, *Nat. Struct. Biol.*, **4**, 578 (1997); b) R. C. Stevens, K. E. Goodwill, C. Sabatier, and F. Fussetti, *J. Inorg. Biochem.*, **67**, 313 (1997); c) H. Erlandsen, F. Fusetti, A. Martinez, E. Hough, T. Flatmark, and R. C. Stevens, *Nat. Struct. Biol.*, **4**, 995 (1997); d) K. E. Goodwill, C. Sabatier, and R. C. Stevens, *Biochemistry*, **37**, 13437 (1998).

9) S. O. Pember, S. J. Benkovic, J. J. Villafranca, M. Pasenkiewicz-Gierula, and W. E. Antholine, *Biochemistry*, **26**, 4477 (1987).

10) R. T. Carr and S. J. Benkovic, *Biochemistry*, **32**, 14132 (1993). During revision of the manuscript, activation of copper-free CVPAH by iron(II) was reported: D. Chen and P. A. Frey, *J. Biol. Chem.*, **273**, 25594 (1998).

11) T. Kohzuma, A. Odani, Y. Morita, M. Takani, and O. Yamauchi, *Inorg. Chem.*, **27**, 3854 (1988).

12) T. Kohzuma, H. Masuda, and O. Yamauchi, *J. Am. Chem. Soc.*, **111**, 3431 (1989).

13) A. Odani, H. Masuda, K. Inukai, and O. Yamauchi, *J. Am. Chem. Soc.*, **114**, 6294 (1992).

14) O. Yamauchi, A. Odani, H. Masuda, and Y. Funahashi, in "Bioinorganic Chemistry of Copper," ed by K. D. Karlin and Z. Tyeklár, Chapman & Hall, New York (1993), p. 363.

15) Y. Funahashi, T. Kohzuma, A. Odani, and O. Yamauchi, *Chem. Lett.*, **1994**, 385.

16) Y. Funahashi, Y. Hara, H. Masuda, and O. Yamauchi, *Inorg. Chem.*, **36**, 3869 (1997).

17) H. I. X. Mager, R. Addink, and W. Berends, *Recl. Trav. Chim. Pays-Bays*, **86**, 833 (1967).

18) W. Pfleiderer and H. Zondler, *Chem. Ber.*, **99**, 3008 (1966).

19) E. L. White, B. L. O'Dell, J. M. Vandenbelt, and J. J. Pfiffner, *J. Am. Chem. Soc.*, **69**, 1786 (1947).

20) R. Mengel and W. Pfleiderer, *Chem. Ber.*, **111**, 3790 (1978).

21) F. M. Jaeger and J. A. Dijk, *Z. Anorg. Chem.*, **1936**, 227.

22) "Single Crystal Structure Analysis Software," Version 1.8 (1997), Molecular Structure Corporation, The Woodlands, TX. 77381.

23) D. T. Cromer and J. T. Waber, in "International Tables for X-Ray Cryatallography," Kyhoch Press., Birmingham (1974), Vol. IV, Table 2.2A, pp. 71—98.

24) a) A. Zuberbühler, *Helv. Chim. Acta*, **50**, 466 (1967); b) A. Zuberbühler, *Helv. Chim. Acta*, **53**, 473 (1970); c) A. Zuberbühler, *Helv. Chim. Acta*, **53**, 669 (1970).

25) R. D. Gray, *J. Am. Chem. Soc.*, **91**, 56 (1969).

26) R. C. Bray, *Biochem. J.*, **81**, 189 (1961).

27) C. P. Poole, Jr., in "Electron Spin Resonance. A Comprehensive Treatise on Experimental Technique," Interscience, New York, p. 776.

28) A. G. Orpen, L. Brammer, F. H. Allen, O. Kennard, D. G. Watson, and R. Taylor, *J. Chem. Soc., Dalton Trans.*, **1989**, S1.

29) M. Bühme, W. Hutzenlaub, W. J. Richter, E. F. Elstner, G. Huttner, J. von Seyerl, and W. Pfleiderer, *Liebigs Ann. Chem.*, **1986**, 1705.

30) a) D. E. Nikles, M. J. Powers, and F. L. Urbach, *Inorg. Chim. Acta*, **37**, L499 (1979); b) V. M. Miskowski, J. A. Thich, R. Solomon, and H. J. Schugar, *J. Am. Chem. Soc.*, **98**, 8344 (1976).

31) H. Masuda, T. Sugimori, T. Kohzuma, A. Odani, and O. Yamauchi, *Bull. Chem. Soc. Jpn.*, **65**, 786 (1992).

32) a) E. W. Ainscough, A. M. Brodie, and N. G. Larsen, *Inorg. Chim. Acta*, **60**, 25 (1982); b) E. W. Ainscough, A. M. Brodie, and N. G. Larsen, *J. Chem. Soc., Dalton Trans.*, **1982**, 815.

33) H. Yokoi and T. Kishi, *Chem. Lett.*, **1973**, 749.
34) J. Peisach and W. E. H. Blumberg, *Arch. Biochem. Biophys.*, **165**, 691 (1974).
35) J. I. Zink and R. S. Drago, *J. Am. Chem. Soc.*, **94**, 4550 (1972).
36) H. Yokoi, M. Sai, and T. Isobe, *Bull. Chem. Soc. Jpn.*, **43**, 1078 (1970).
37) T. Sawada, K. Fukumaru, and H. Sakurai, *Biochem. Biophys. Res. Commun.*, **216**, 154 (1995).
38) U. Sakaguchi and A. W. Addison, *J. Am. Chem. Soc.*, **99**, 5189 (1977).
39) U. Sakaguchi and A. W. Addison, *J. Chem. Soc., Dalton Trans.*, **1979**, 600.
40) R. S. Nicholson and I. Shain, *Anal. Chem.*, **36**,706 (1964).
41) J. Perkinson, S. Brodie, K. Yoon, K. Mosny, P. J. Carroll, T. V. Morgan, and S. J. N. Burgmayer, *Inorg. Chem.*, **30**, 719 (1991).
42) R. A. Lazarus, R. F. Dietrich, D. E. Wallick, and S. J. Benkovic, *Biochemistry*, **20**, 6834 (1981).
43) D. Ege-Serpkenci and G. Dryhurst, *Bioelectrochem. Bioenerg.*, **9**, 175 (1982).
44) J. F. Boas, R. H. Dunhill, J. R. Pilbrow, R. C. Srivastava, and T. D. Smith, *J. Chem. Soc. A*, **1969**, 94.
45) M. Vicontini and A. Bobst, *Helv. Chim. Acta*, **49**, 1815 (1966).
46) M. C. Archer, D. J. Von der Schmitt, and K. G. Scrimgeour, *Can. J. Biochem.*, **50**, 1174 (1972).
47) D. E. Wallick, L. M. Bloom, B. J. Gaffney, and S. J. Benkovic, *Biochemistry*, **23**, 1295 (1984).